phycology

MDPI

Article

Microalgal Communities in Mucilage Aggregates (Northern Adriatic Sea, Summer 2024) Based on Microscopy and Metabarcoding

Marika Ubaldi [1,2,3], Francesca Neri [3,*], Giorgia Montali [3], Tiziana Romagnoli [3], Aurora Tomasini [3], Federica Cerino [2,4], Timotej Turk Dermastia [5], Patricija Mozetič [5], Janja Francé [5], Camilla Spoto [6], Stefano Accoroni [3,*] and Cecilia Totti [3]

1 Department of Marine and Earth Science, Università degli Studi di Palermo, Via Archirafi 22, 90123 Palermo, Italy; m.ubaldi@univpm.it
2 NBFC—National Biodiversity Future Center, Piazza Marina 61, 90133 Palermo, Italy; fcerino@ogs.it
3 Department of Life and Environmental Sciences, Polytechnic University of Marche, Via Brecce Bianche, 60131 Ancona, Italy; s1112616@studenti.univpm.it (G.M.); t.romagnoli@univpm.it (T.R.); a.tomasini@staff.univpm.it (A.T.); c.totti@univpm.it (C.T.)
4 Section of Oceanography, Institute of Oceanography and Applied Geophysics—OGS, Via Auguste Piccard 54, 34151 Trieste, Italy
5 Marine Biology Station Piran, National Institute of Biology, Fornače 41, 6330 Piran, Slovenia; timotej.turkdermastia@nib.si (T.T.D.); patricija.mozetic@nib.si (P.M.); janja.france@nib.si (J.F.)
6 Department of Life Sciences, University of Trieste, 34128 Trieste, Italy; camilla.spoto@units.it
* Correspondence: f.neri@pm.univpm.it (F.N.); s.accoroni@univpm.it (S.A.)

Abstract

The mucilage phenomenon consists of the appearance of large gelatinous aggregates floating in the water column. In summer 2024, this event has reappeared in the Northern Adriatic Sea (NAS) on a large scale. This study provides an integrated characterization of the microalgal community within mucilage aggregates and surrounding waters in two NAS areas (Gulf of Trieste and Conero Riviera) using light microscopy (LM), metabarcoding (MB) based on ribosomal 18S V4 and V9 markers, and scanning electron microscopy (SEM) for selected taxa identification. Mucilage aggregates acted as dynamic microbial hotspots, hosting a rich diatom community, with abundances 1–2 orders of magnitude higher than in the surrounding water. Dominant diatom species were *Cylindrotheca closterium*, *Nitzschia* spp., *Nitzschia gobbii*, and *Thalassionema nitzschioides*. Some phytoflagellates (e.g., *Tetraselmis* spp.) and dinoflagellates (e.g., *Karlodinium veneficum*, *Pseliodinium fusus*, and *Wangodinium sinense*) were detected exclusively by MB, while LM and SEM revealed species missed by other approaches. *Gonyaulax fragilis*, one of the species indicated as an important mucus producer, was present at the onset and throughout the phenomenon, as detected by LM and MB. The integrated approach improves knowledge of microalgal communities in NAS mucilage.

Keywords: mucilage; Northern Adriatic Sea; phytoplankton; microalgae; metabarcoding; microscopy; *Gonyaulax fragilis*; Harmful Algal Blooms

Academic Editor: Leonel Pereira

Received: 29 November 2025
Revised: 22 December 2025
Accepted: 24 December 2025
Published: 1 January 2026

1. Introduction

The Northern Adriatic Sea (NAS) is the northernmost basin of the Mediterranean Sea. Its productivity varies across the basin and is strongly influenced by inputs of nutrient-rich riverine waters, primarily the Po River [1–4], resulting in conditions ranging from

eutrophic to oligotrophic [5]. Moreover, it is characterized by a dominant cyclonic circulation and a shallow depth [6]. This area has been historically characterized by a number of harmful events related to microalgal communities including Harmful Algal Blooms (HABs), with proliferations of toxic microalgal species [7] and associated shellfish contamination by toxins [8,9], red tides [10], eutrophication, oxygen depletion, and the mucilage formation [5,11–16].

Mucilage occurrence, also known as the "dirty sea" phenomenon, consists of the appearance of huge gelatinous aggregates of microalgal origin in the water column (pelagic mucilage). Although mucilage aggregates are not toxic, they can negatively impact marine ecosystems [17] and economic activities, as they smother benthic species, hinder fisheries and aquaculture by clogging nets, and affect tourism by discouraging bathing [18]. Moreover, sometimes mucilage phenomena have been associated with benthic hypoxia [2], and recent studies suggest they can also induce oxidative stress in marine organisms, affecting key antioxidant defenses [19]. Mucilage aggregates can be very different in size and morphology and have therefore been classified according to their structural form and their spatial distribution along the water column into five stages: marine snow (flocs and macroflocs), stringers, clouds, creamy surface layer, and gelatinous surface layer [14,15].

The occurrence of mucilage was first reported in the NAS in 1729 [20], followed by further occurrences in 1872, 1880, 1891, 1901, 1903, 1905, 1920, 1921, 1924, 1927, 1929, 1930, 1941, 1949, 1973, 1983, 1984, and 1986 [18,21]. More recently, events of mucilage macroaggregate formation occurred in 1988, 1989, 1991, 1997, 2000, 2002, 2004, 2014, and 2018 [18,22]. Documented occurrences over time are summarized in Figure 1.

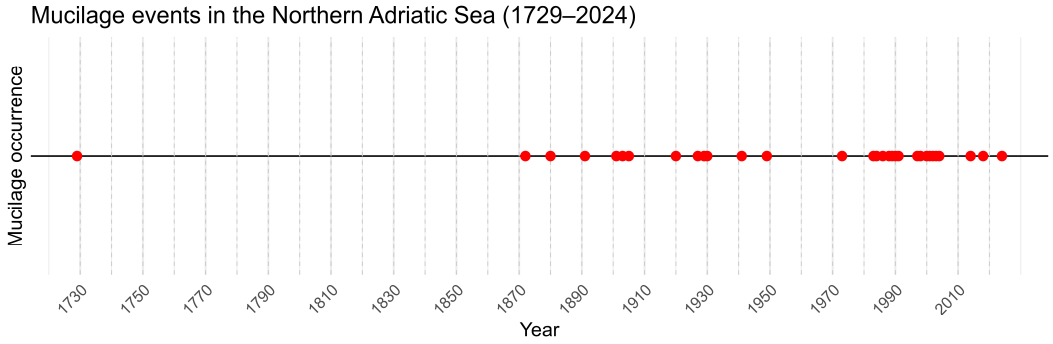

Figure 1. Historical occurrences of mucilage events in the NAS (1729–2024) based on published records. Red dots indicate the years in which mucilage events occurred.

Initially, it was suspected that the species that were most abundant in the mucus under the microscope were responsible for the phenomenon, although the composition of the samples varied greatly among areas, and several species have been considered potential producers, including benthic diatoms, pelagic diatoms, and dinoflagellates [20].

An enormous study program occurred in the 2000s, to study this phenomenon from different points of view [18], and many interrogatives were resolved. Mucilage composition consists mainly of water (90–99%); the remaining dry mass consists of 30–60% organic matter such as polysaccharides (the primary component), proteins and lipids, and an inorganic fraction made up of salts containing macroelements and trace microelements [23–25].

It is noticeable that mucilage aggregates are refractory to the degradation, and this explains their long persistence [26–28]. As regards the biological component, mucilage aggregates represent optimal microenvironments that support a rich community of microorganisms like diatoms, dinoflagellates, bacteria, cyanobacteria, etc., which reach abundances 1–2 orders of magnitude higher than in the surrounding water [29,30].

Mucilage production is a complex phenomenon that has been widely reviewed in the literature and has been linked to a combination of causes, including the oceanographic con-

ditions that take place in the NAS during late-spring/summer, such as a reduced circulation, strong stratification of the water column and high atmospheric pressure, which facilitate mucilage aggregate accumulation and stabilization [11,14,31,32]. Rising sea temperatures due to global warming could exacerbate the phenomenon [32,33]. Atmospheric factors such as strong winds or storm surges can interrupt or reduce mucilage development [31].

Many studies converged in recognizing that the mucilage formation is mainly due to the excretion of polysaccharides by microalgae under stressed environmental conditions [34–38]. Diatom species have been suspected as possible causes of the phenomenon, as they occur abundantly in mucilage and have been reported to produce high amounts of extracellular polysaccharides, especially under an unbalanced N/P ratio [39,40]. However, many authors have increasingly recognized the important role of the dinoflagellate *Gonyaulax fragilis* (F. Schütt) F. Kofoid (Dinophyceae) in the phenomenon. Pompei et al. (2003) [41] reported that NAS mucilage is correlated mainly with the presence and growth of *Gonyaulax fragilis* considering that just a few thousand *Gonyaulax fragilis* cells release the same amount of carbohydrates as that excreted by tens of millions of *Cylindrotheca closterium* (Ehrenberg) Reimann and J.C. Lewin (Bacillariophyceae) cells [42,43].

Pelagic mucilage occurrence is well documented not only in the NAS but also in other areas worldwide. In the Sea of Marmara, where such events have been frequently reported (e.g., in 2007 and, more recently, in 2021 as a very large event [34]), *Gonyaulax fragilis* is indicated among the suspected species [34,36,44]. In the Aegean Sea, mucilage has been linked to blooms of *Gonyaulax fragilis* [45]. In New Zealand, this phenomenon, reported as marine slime [35,46], has also been linked to polysaccharide exudates released by *Gonyaulax hyaline*, a species now synonymized with *G. fragilis* [35].

Similar events, though with a completely different origin, are the benthic mucilage events reported in the Tyrrhenian Sea since 1991, which have been produced by benthic chrysophytes and/or ectocarpalean brown algae [47].

Since the initial observations of mucilage events, considerable attention has been given to the composition of microalgal communities within mucus compared to the surrounding water, as these organisms may play a role in the early stages of the phenomenon [20]. Comparative analysis using metagenomic approaches have also been conducted to characterize the microbial community inside and outside the aggregates [48].

In actuality, a number of studies about the diversity of microalgae associated with mucilage based on microscopic observations are available [13–15,21,25,29,34–36,41,45,49–53], but there are few studies using metabarcoding approaches [54,55]. Indeed, traditionally, microalgal communities have been studied through inverted light microscopy. This method is important because it provides information about community composition, abundance, and biomass. Nevertheless, this approach presents some limitations: it is time-consuming, requires an expert taxonomist and shows difficulty in distinguishing morphologically cryptic, rare, or small species. This can be compensated for by the metabarcoding approaches; however, they provide only relative abundance information, and the accuracy of the taxonomic assignment depends on the completeness and accuracy of the available reference databases [56]. Therefore, an increasing number of studies have integrated microscopy and metabarcoding approaches to study the phytoplankton biodiversity [57–59].

During the summer of 2024, a new event of mucilage phenomenon reoccurred in the NAS. The first appearance was observed in early June along the western Istrian coastline (from Brijuni to Piran) [32]. Then, following the counterclockwise circulation, it moved through the Gulf of Trieste, the Venice Lagoon, and the coasts of Emilia Romagna and Marche, reaching as far south as Apulia.

This study, conducted in two areas of the Northern Adriatic Sea (Conero Riviera and Gulf of Trieste) affected by the 2024 mucilage event, aims to (i) investigate the abundance

and biodiversity of microalgae in the mucilage and surrounding water samples by combining microscopy and metabarcoding analysis to gain a deeper understanding of the dynamics of microalgal communities during the appearance of mucilage aggregates and (ii) assess the evolution of microalgal composition during the mucilage event.

2. Materials and Methods

2.1. Sampling Area and Sample Collection

Sampling was conducted in the NAS, specifically in the Gulf of Trieste and in the Conero Riviera (Figure 2), between June and August 2024 (Table 1). In the Gulf of Trieste, sampling was carried out at 00BF (45°32′55.8″ N, 13°33′1.8″ E), C2 (45°34′48.0″ N, 13°36′48.0″ E), and C1-LTER (45°42′2.99″ N, 13°42′36.0″ E), while in the Conero Riviera samples were collected at Portonovo (43°36′12.06″ N, 13°36′42.3″ E) and Passetto (43°37′09″ N, 13°31′54″ E).

Table 1. Overview of sampling activities conducted during the mucilage phenomenon. For each sample the sampling date, station name, type of sample collected (mucilage or surrounding water), and type of analysis performed (LM, SEM, MB) are reported.

Date	Station	Sample Type	Analysis
27 June 2024	Portonovo (Conero Riviera)	Mucilage	LM and MB V4–V9
1 July 2024	Passetto (Conero Riviera)	Mucilage	MB V4–V9
5 July 2024	00BF (Gulf of Trieste)	Mucilage	MB V4
5 July 2024	00BF (Gulf of Trieste)	Surrounding water	LM
9 July 2024	C2 (Gulf of Trieste)	Mucilage	MB V4
11 July 2024	Passetto (Conero Riviera)	Mucilage	LM and MB V4–V9
11 July 2024	Passetto (Conero Riviera)	Surrounding water	LM and MB V4–V9
12 July 2024	Passetto (Conero Riviera)	Mucilage	LM and MB V4–V9
12 July 2024	Passetto (Conero Riviera)	Surrounding water	LM and MB V4–V9
16 July 2024	C1-LTER	Mucilage	LM and MB V4
16 July 2024	C1-LTER	Surrounding water	LM and MB V4
19 July 2024	00BF	Mucilage	MB V4
19 July 2024	00BF	Surrounding water	LM and MB V4
21 July 2024	Passetto (Conero Riviera)	Mucilage	LM and MB V4–V9
21 July 2024	Passetto (Conero Riviera)	Surrounding water	LM and MB V4–V9
9 August 2024	Passetto (Conero Riviera)	Mucilage	LM, SEM and MB V4–V9
9 August 2024	Passetto (Conero Riviera)	Surrounding water	LM, SEM and MB V4–V9

During each sampling, the mucilage and/or surrounding water were collected for light microscopy (LM), metabarcoding (MB), and/or scanning electron microscopy (SEM) as summarized in Table 1. Samples of both matrices were taken at different depths depending on the position of mucus aggregates in the water column, eventually with the assistance of SCUBA divers using syringes. Mucilage samples were then transferred to sterile Falcon tubes for MB analysis.

All samples for LM, whether mucilage or seawater, were fixed with prefiltered and neutralized formaldehyde at a final concentration of 0.8–2% [60] and stored in the dark until analysis. For MB, both the sample types from Conero Riviera and C1-LTER stations, 50 mL of the samples were filtered using cellulose nitrate filters (47 mm diameter, 1.2 µm pore-size, Sartorius) and stored in the laboratory at −20 °C until DNA extraction. The samples from 00BF and C2 stations were processed differently: two replicates of 1 L surrounding water were filtered through 0.8 µm polycarbonate filters, while three 1.8 mL replicates of mucilage were pipetted as accurately as possible into microcentrifuge tubes without filtration. All samples were stored at −80 °C until DNA extraction.

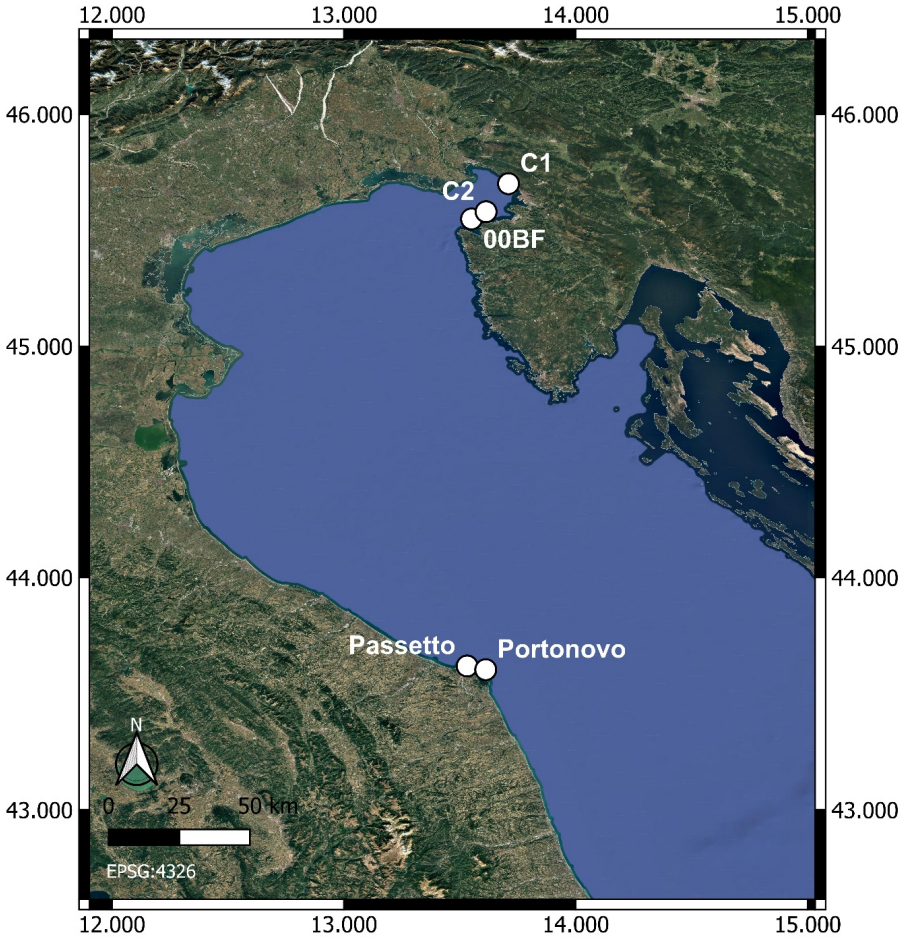

Figure 2. Map of the study area in the Northern Adriatic Sea with the following sampling sites: Conero Riviera including Portonovo and Passetto (Ancona, Italy) and 00BF and C2 (Piran, Slovenia) and C1-LTER (Trieste, Italy) in the Gulf of Trieste.

2.2. Metabarcoding Analysis

DNA was extracted using the DNeasy PowerWater Kit (QIAGEN, Hilden, Germany) following the manufacturer's instructions. The filters were cut in half, each half was extracted separately and then pooled after elution based on Neri et al. [58]. Mucilage samples from stations 00BF and C2, which were pipetted (1.8 mL) and stored in microcentrifuge tubes, were homogenized in the tubes using a hand-held homogenizer and sterile plastic pestles. DNA was extracted from the resulting homogenate using the E.Z.N.A. Mollusc DNA Kit (Omega-Biotec, Norcross, GA, USA) according to the manufacturer's guidelines. The concentration of all DNA extracts was measured using a NanoDrop spectrophotometer (Thermo Fisher Scientific, Waltham, MA, USA). For amplification, the hypervariable V4 and V9 regions of the universal 18S rRNA gene were selected, as they are widely used in microalgal metabarcoding studies due to their broad taxonomic coverage and resolution, which typically allows identification at genus level and/or species level for some taxa, owing to their high representation in reference databases [58,59,61,62]. For samples collected at the Conero Riviera station, both the V4 and V9 regions were targeted, while for the Gulf of Trieste stations, only the V4 region was targeted. PCR amplification and sequencing for samples from Conero Riviera stations and from 00BF and C2 stations of the Gulf of Trieste were carried out by Beijing Novogene Biotechnology Co., Ltd. (Beijing, China) using the Illumina paired-end sequencing (PE250, 2 × 250 bp) format. Instead, samples from the C1-LTER station of the Gulf of Trieste were processed by BMR Genomics (Padova, Italy) using MiSeq platform in the paired-end 2 × 300 bp format. For PCR amplification, primers

from Piredda et al. (2017) [59] were used (V4 18S F: CCAGCASCYGCGGTAATTCC and V4 18S R: ACTTTCGTTCTTGATYRATGA; V9 18S F: TTGTACACACCGCCCGTCGC and V9 18S R: CCTTCYGCAGGTTCACCTAC) [58], giving amplicons of ∼230 bp for V4 and ∼130 bp for V9.

The quality of each raw read and presence of adapter sequences were assessed using FASTQC (v. 0.11.9) [63]. Primer trimming was performed using cutadapt (v. 4.5) [64]. The processing and analyzing of raw reads from all the sampling stations were performed using QIIME2 (v. 2024.2) [65] and a quality control step, including filtering, denoising, and merging of paired-end reads, was conducted with the DADA2 plugin implemented within QIIME2 [66]. Denoising and quality filtering of each dataset were performed independently due to differences in sequencing providers and run-specific conditions. After denoising, representative sequences were merged in QIIME 2 to allow consistent taxonomic assignment of amplicon sequence variants (ASVs) across all datasets. Taxonomic classification was carried out in QIIME 2 using a Naïve Bayes classifier [67] with default parameters trained on 18S rRNA gene target regions (V4 and V9), using reference sequences from the PR2 database (v5.1.0) [68] and SILVA database (v138.2) [69].

2.3. Microscopy Analysis

Microalgae identification and counting of both sample types (mucilage and surrounding water) were conducted using an inverted light microscope equipped with phase contrast, following the Utermöhl method [70]. Cell counts were performed at 400× magnification in variable number of random visual fields or in transects, depending on cell abundance. To improve the detection of larger and less abundant species, one half or the entire Utermöhl chamber was analyzed at 200× magnification. A different approach was used for mucilage samples collected at stations 00BF and C2. As the material was very dense and gelatinous, settling in a Utermöhl chamber was not possible. Instead, a drop or piece of mucilage was placed on a microscope slide, covered with a cover slip, and observed under an inverted microscope. Magnifications ranged from 200× to 1000× using immersion oil. A few sub-samples from each sample were qualitatively analyzed, with annotations for the most abundant species.

Taxa were identified to the lowest possible taxonomic level and subsequently grouped into four phytoplankton groups: diatoms, dinoflagellates, coccolithophores, and phytoflagellates. The category 'phytoflagellates' included all flagellate groups that could not be identified under LM, often not even to the class level, including haptophytes (excluding coccolithophores), cryptophytes, chrysophytes, dictyochophytes, raphidophytes, chlorophytes, and euglenophytes. Most taxa within these groups have been always classified as 'undetermined phytoflagellates' and could include also heterotrophic taxa, as LM analysis does not allow one to discriminate between autotrophic and heterotrophic organisms.

To identify problematic taxa, sub-samples from the Passetto station (Conero Riviera) collected on 9 August 2024 were used for ultrastructural analysis by scanning electron microscopy (SEM). For diatoms, preserved sub-samples were acid-cleaned following the von Stosch protocol [71] and a drop of the cleaned suspension was placed on a stub. For dinoflagellates, preserved sub-samples (1 mL) were filtered on a Nucleopore polycarbonate filter using a Swinnex filter holder and a syringe. The filters where then dehydrated by immersion in ethanol increasing gradations (10, 30, 50, 70, 80, 90, 95, and 100%). After 1 day in absolute ethanol, the dehydrated samples were treated in a Critical Point Dryer (Polaron CPD7501, Quorum Technologies, Newhaven, UK) and filters were mounted on stubs. Both stubs, for diatom and dinoflagellate samples, were sputter-coated with gold-palladium in a Sputter Coater (Polaron SC 7640). Both samples were visualized under a scanning electron microscope, specifically, a Zeiss Supra 40 FE-SEM (Carl Zeiss AG, Oberkochen, Germany).

2.4. Data Analysis

Taxonomic names in the datasets obtained with both methods were corrected and updated by cross-referencing with AlgaeBase [72] to ensure accuracy and consistency. Additionally, the dataset obtained through MB was curated by removing taxa irrelevant to our study objectives, such as fungi, bacteria, and other non-target taxonomic groups (e.g., Metazoa and macroalgae), using the R package phyloseq (version 4.3.1) [73]. In cases of taxonomic uncertainty, such as ASVs corresponding to unusual or unexpected species not previously recorded in the study area, identifications were validated using the NCBI nucleotide database (Genbank) with BLASTn online tool (https://blast.ncbi.nlm.nih.gov, accessed on 1 November 2025) [74] with default parameters, and any incorrect assignments were either corrected or excluded. To improve consistency and comparability between MB and LM, the 'phytoflagellates' category in the MB dataset was expanded to include additional taxa that, under LM, are morphologically indistinguishable from phytoflagellates. This adjustment accounts for the fact that LM may also include small heterotrophic cells with a similar morphology in the phytoflagellates counts.

Due the stochastic nature of this phenomenon, the sampling design was not fully balanced. Therefore, comparisons between mucilage and surrounding water were restricted to sampling dates for which both sample types were available. Specifically paired samples for LM were collected at Passetto (11 July, 12 July, 21 July, and 9 August) and at C1-LTER (16 July). LM data obtained from these paired samples were used to estimate total microalgal abundance, calculate alpha diversity indices, and generate Venn diagrams of unique and shared species between the mucilage and surrounding water. Alpha diversity was estimated using the Shannon and Simpson diversity indices computed with the vegan package in R [75]. Differences between the two sample types were visualized using boxplots and statistically tested with the Wilcoxon rank-sum test with a p-value < 0.05 considered statistically significant. For MB data, comparative Venn diagram analyses were conducted using mucilage samples collected at 00BF (19 July), C1-LTER (16 July), and Passetto (11 July, 12 July, 21 July, and 9 August), together with the corresponding surrounding water samples collected on the same dates.

Bar plots were used to show changes in the most abundant species identified by LM and in phytoplankton groups in the two study areas based on MB data, while bubble plots were used to visualize the most abundant species detected by MB. All bar and bubble plots based on LM and MB data were generated using all the available mucilage and surrounding water samples.

All statistical analyses were performed using RStudio (version 4.3.1) [76] and all graphics were generated with the ggplot2 package [77].

3. Results

Qualitative and quantitative analysis of the mucilage under LM revealed a high abundance of *Gonyaulax fragilis* at the onset and during the phenomenon (Figure 3a), whereas towards the end, many of its broken thecae or only few were observed. The abundances of *Gonyaulax fragilis* were 6.93×10^5 cells/L on 27 June at Portonovo station, reaching a maximum of 2.16×10^6 cells/L at of Passetto station on 12 July. Among diatoms, several species dominated in mucilage samples, mainly *Thalassionema nitzschioides* (Grunow) Mereschkowsky, (Bacillariophyceae), *Nitzschia gobbii* (Accoroni, Romagnoli, Giulietti and Totti), (Bacillariophyceae), *Nitzschia* spp. (Bacillariophyceae), and *Cylindrotheca closterium* (Figure 3b). These most abundant diatoms reached their highest abundances in the mucilage at Passetto station on 21 July. Specifically, *Thalassionema nitzschioides* reached 1.97×10^7 cells/L in the mucilage (compared to 2.63×10^4 cells/L in the surrounding water), *Nitzschia gobbii* reached 3.57×10^7 cells/L in the mucilage (versus 8.54×10^4 cells/L

in the surrounding water), and *Cylindrotheca closterium* reached 5.14 × 10^6 cells/L in the mucilage (compared to 2.50 × 10^3 cells/L in the surrounding water). Other species observed at lower abundances included *Cerataulina pelagica* (Cleve) Hendey (Mediophyceae), *Chaetoceros diversus* Cleve, (Mediophyceae), *Dactyliosolen blavyanus* (H. Peragallo) Hasle (Coscinodiscophyceae), *Dactyliosolen fragilissimus* (Bergon) Hasle (Coscinodiscophyceae), *Gephyrocapsa huxleyi* (Lohmann) P. Reinhardt (Coccolithophyceae), *Gonyaulax polygramma* F. Stein (Dinophyceae), *Leptocylindrus danicus* Cleve (Mediophyceae), *Licmophora abbreviata* C. Agardh (Bacillariophyceae), *Licmophora flabellata* (Greville) C. Agardh (Bacillariophyceae), *Nitzschia longissima* (Brébisson ex Kützing) Grunow (Bacillariophyceae), *Oxytoxum scolopax* F. Stein (Dinophyceae), *Paulinella ovalis* P.W. Johnson, Hargraves and Sieburth (Imbricatea), *Podolampas bipes* F. Stein (Dinophyceae), *Proboscia alata* (Brightwell) Sundström (Mediophyceae), *Prorocentrum micans* Ehrenberg (Dinophyceae), *Protoperidinium bipes* (Paulsen) Balech (Dinophyceae), *Pseudo-nitzschia pseudodelicatissima* complex, *Skeletonema marinoi* Sarno and Zingone (Mediophyceae), *Striatella unipunctata* (Lyngbye) C. Agardh (Bacillariophyceae), and several *Tripos* species. Their abundances were generally lower than the dominant species, ranging from 4.17 × 10^2 cells/L to 4.60 × 10^6 cells/L, depending on the species and sampling date.

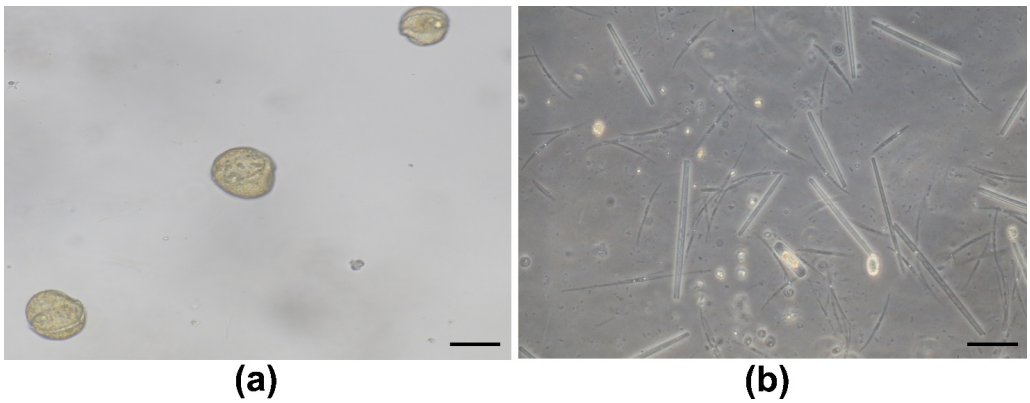

Figure 3. LM images of mucilage samples: (**a**) sample collected on the Conero Riviera on 6 June 2024 showing *Gonyaulax fragilis* and (**b**) sample collected on the Conero Riviera on 9 August 2024 showing a very diversified diatom community (mainly *Thalassionema nitzschioides*, *Nitzschia gobbii*, *Nitzschia* spp.). Scale bars: 50 μm.

The taxa examined with SEM, both in the surrounding water and mucilage samples (Figure 4), confirmed the identification of the most abundant species, i.e., *Cylindrotheca closterium*, *Nitzschia* sp., *Thalassionema nitzschioides*, and, in addition, *Nitzschia longissima*. Furthermore, some less abundant taxa found in both sample types were *Amphora* sp. (Bacillariophyceae), *Cyclotella* sp. (Bacillariophyceae), *Cocconeis euglypta* Ehrenberg (Bacillariophyceae), *Diploneis* sp. (Bacillariophyceae), *Licmophora* sp. (Bacillariophyceae), *Navicula perminuta* Grunow (Bacillariophyceae), *Pleurosigma* sp. (Bacillariophyceae), *Scrippsiella rotunda* (Dinophyceae), and *Nanofrustulum* sp. (Bacillariophyceae) (Figure 5).

3.1. Comparison Between Mucilage Aggregates and Surrounding Water

Microalgal total abundances obtained by LM in mucilage samples showed values 1–2 orders of magnitude higher (Wilcoxon test, $p < 0.05$) than in the surrounding water (Figure 6). The lowest mucilage abundance was later recorded on 16 July (4.53 × 10^6 cells/L) at the C1-LTER station, when the surrounding water contained 1.08 × 10^6 cells/L. The maximum abundance in mucilage was recorded at Passetto station on 21 July (1.37 × 10^8 cells/L), while the surrounding water on the same date had

3.48×10^5 cells/L. Finally, the highest abundance in the surrounding water was measured at Passetto station on 9 August (1.91×10^7 cells/L).

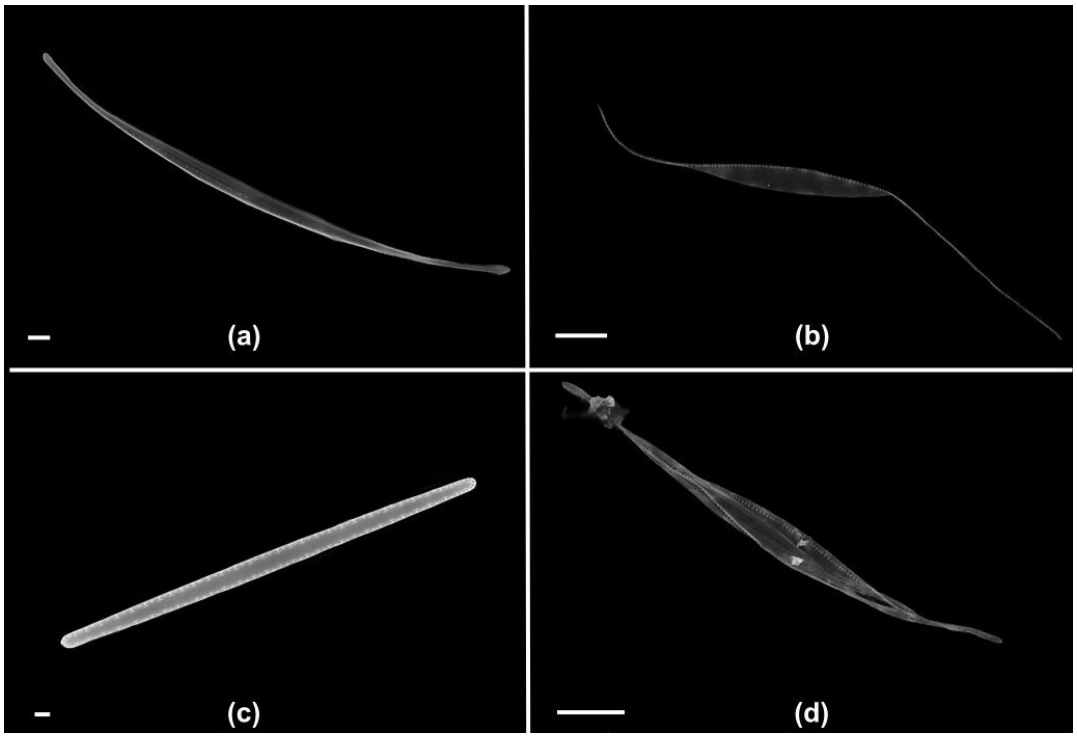

Figure 4. SEM images of most abundant taxa from mucilage and surrounding water samples from Conero Riviera: (**a**) = *Nitzschia* sp., scale bar = 2 µm; (**b**) = *Nitzschia longissima*, scale bar = 10 µm; (**c**) = *Thalassionema nitzschioides*, scale bar = 2 µm; and (**d**) = *Cylindrotheca closterium*, scale bar = 10 µm.

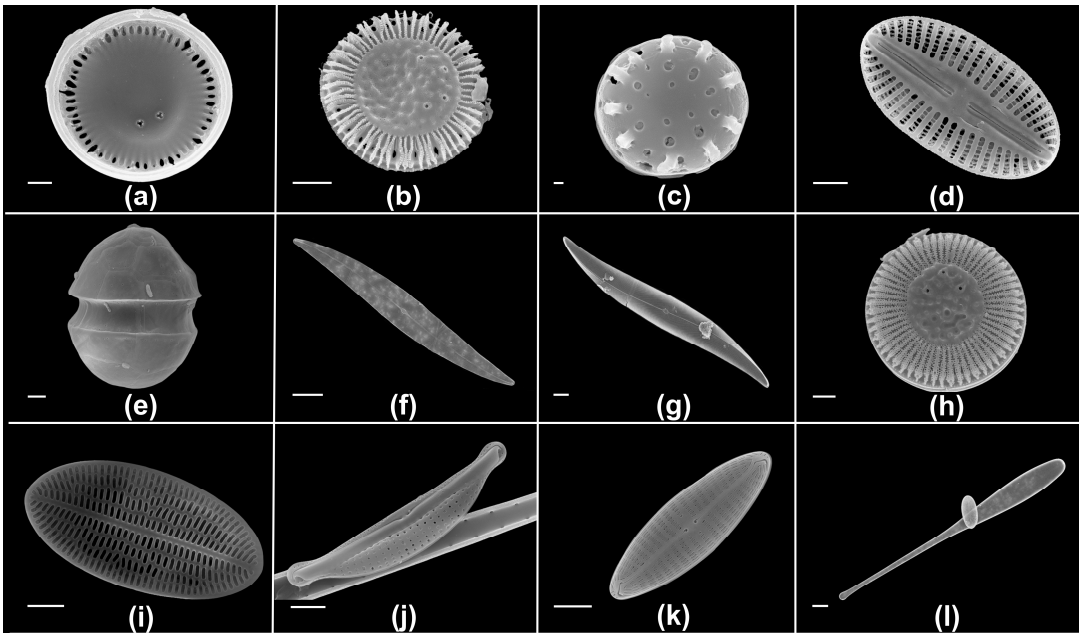

Figure 5. SEM images of less abundant taxa from mucus samples (**a**–**f**) and from surrounding water samples (**g**–**l**) from Conero Riviera: (**a**) *Cyclotella* sp. internal valve view, (**b**) *Cyclotella* sp. external valve view, (**c**) *Nanofrustulum* sp., (**d**) *Diploneis* sp. internal valve view, (**e**) *Scrippsiella rotunda*, (**f**) *Pleurosigma* sp., (**g**) *Pleurosigma* sp., (**h**) *Cyclotella* sp. external valve view, (**i**) *Cocconeis euglypta* (**j**) *Amphora* sp., (**k**) *Navicula perminuta*, and (**l**) *Licmophora* sp. (**a**) Scale bar = 1 µm; (**b**,**d**,**e**,**i**–**k**) scale bar = 2 µm; (**c**) scale bar = 200 nm; (**f**–**h**,**l**) scale bar = 10 µm.

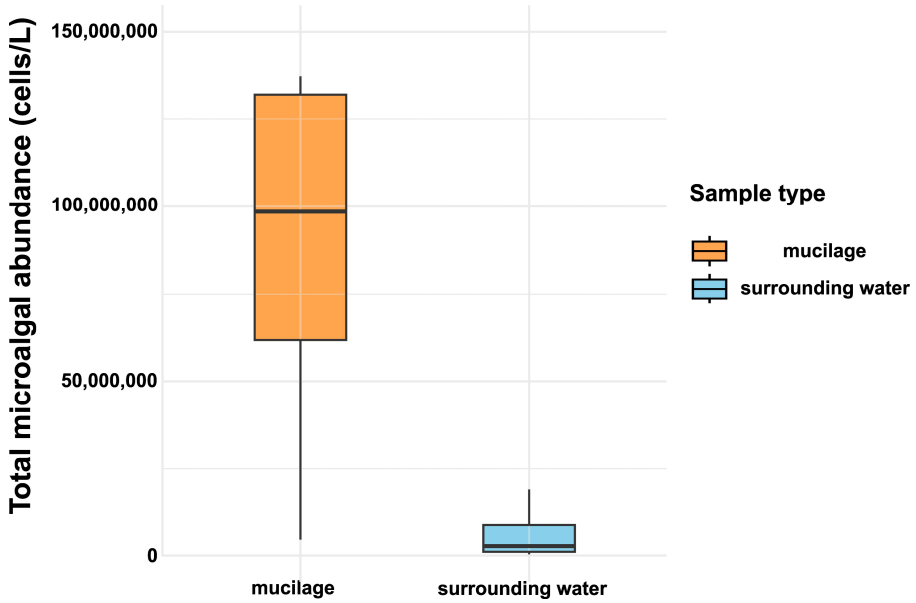

Figure 6. Boxplots of the total microalgal abundance (cells L^{-1}) in mucilage aggregates (orange) and surrounding seawater (light blue) samples. Data from LM analyses.

LM showed that diatoms and phytoflagellates were the most abundant groups in both sample types (Supplementary Table S1). In the mucilage samples diatoms ranged from 4.38×10^7 cells/L (43.2%) to 6.58×10^7 cells/L (66.8%), whereas in the surrounding water they ranged from 8.23×10^4 (47%) to 1.40×10^7 (73.39%). Phytoflagellates abundances in the mucilage ranged from 5.54×10^7 (54.4%) to 3.19×10^7 cells/L (32.4%), while in the surrounding water they ranged from 6.20×10^4 (35.5%) to 4.87×10^6 (25.4%).

Both Simpson (Figure 7a) and Shannon diversity indices (Figure 7b) showed no statistically significant differences in diversity between the mucilage samples and the surrounding water (Wilcoxon test, $p > 0.05$).

Venn diagrams, obtained by LM analyses, identified 35.3% of unique species in the surrounding water, 17.6% unique in the mucilage, and 47.1% of species shared between the two sample types (Figure 8a). Specifically, 34 species were found, including 19 diatoms, 9 dinoflagellates, 2 coccolithophores, and 4 phytoflagellates (Supplementary Table S2). These results are consistent with those obtained through MB. Venn diagrams based on MB showed the overlap in terms of microalgal species (Figure 8b) and genera (Figure 8c) identified in mucilage and surrounding water samples, using the V4 and V9 markers and PR2 and SILVA databases. A higher number of unique species were detected in the surrounding water compared to mucilage, with 124 and 67 species, respectively. Also at the genus level, higher number of unique genera was detected in the surrounding water compared to mucilage, with 86 and 62 genera, respectively. A total of 105 species and 155 genera were shared between the two sample types. Overall, 294 species (67 diatoms, 71 dinoflagellates, 5 coccolithophores, and 151 phytoflagellates) (Supplementary Table S2) and 303 genera (55 diatoms, 63 dinoflagellates, 4 coccolithophores, and 181 phytoflagellates) (Supplementary Table S3) were identified across all methodological MB approaches.

3.2. Evolution of Microalgal Composition in Mucilage and Surrounding Water

LM analyses focusing on the 10 most abundant species in mucilage (Figure 8a) and surrounding water samples (Figure 9b) highlighted the presence of *Gonyaulax fragilis* in mucilage on the first weeks of the phenomenon. After, a decrease over time was observed, accompanied by an increase in the relative abundance of *Nitzschia gobbii* at the beginning and of *Thalassionema nitzschioides* towards the end. This trend was clearly observed in

both mucilage and water samples, with the only difference being that in the water column abundances were much lower. It is noteworthy that *Gonyaulax fragilis* was not found among the 10 most abundant species in the surrounding water samples.

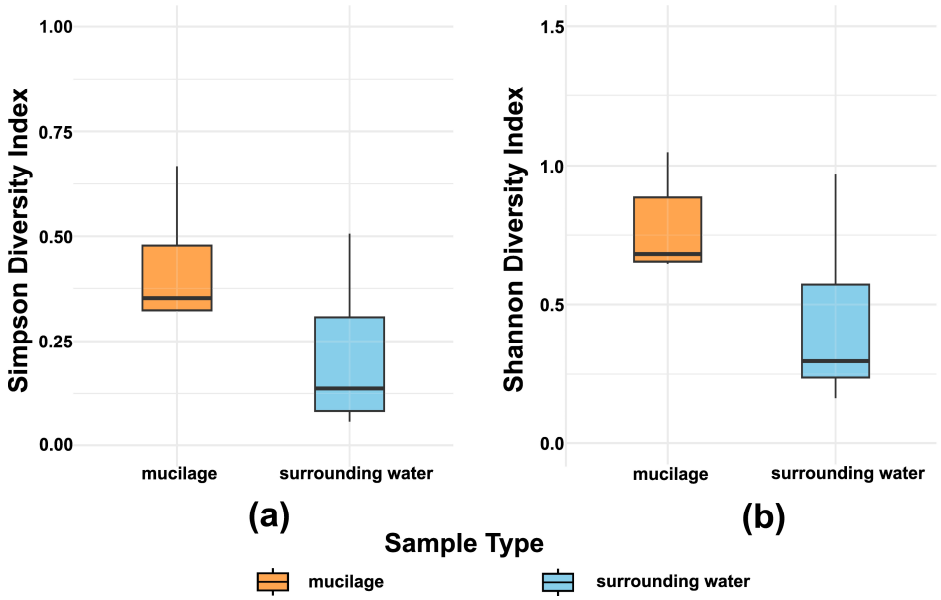

Figure 7. Simpson (**a**) and Shannon (**b**) diversity indices of microalgae in mucilage samples (orange plot) and surrounding water (light blue) observed by LM. Although higher values were observed in mucilage samples, the differences were not statistically significant.

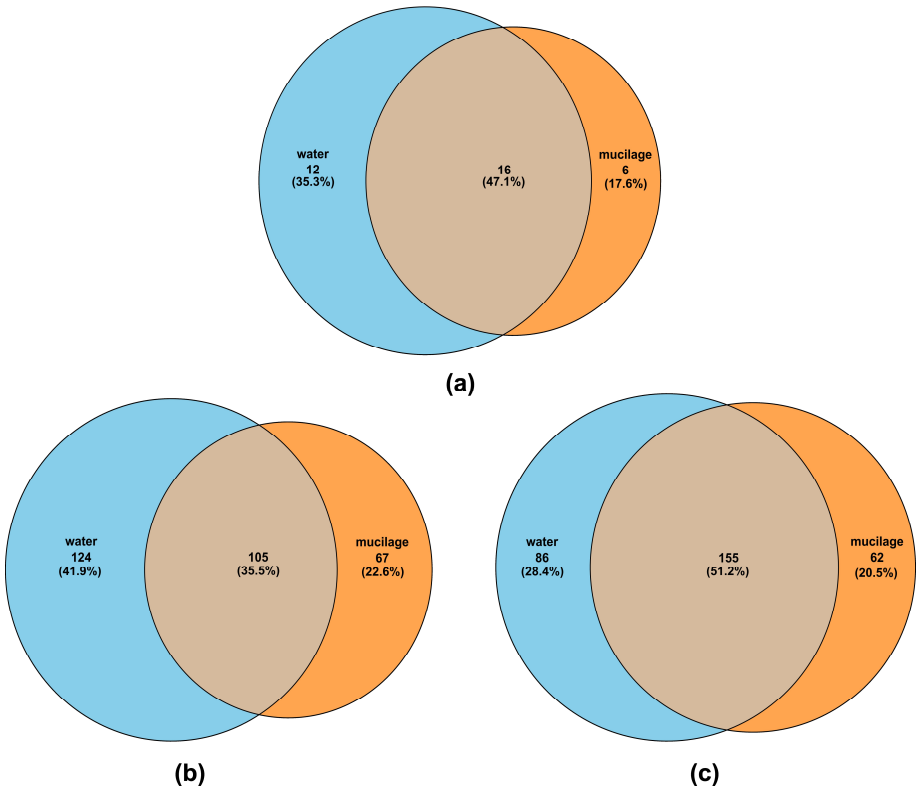

Figure 8. Venn diagrams showing the number (and percentage) of shared and unique microalgae species from LM analysis (**a**) and shared and unique microalgae species (**b**) and genera (**c**) based on results integrating all metabarcoding approaches, V4 and V9 markers and PR2 and SILVA databases for taxonomic assignment, between mucilage (orange) and surrounding water (light blue) samples. Brown areas indicate taxa shared between the two sample types.

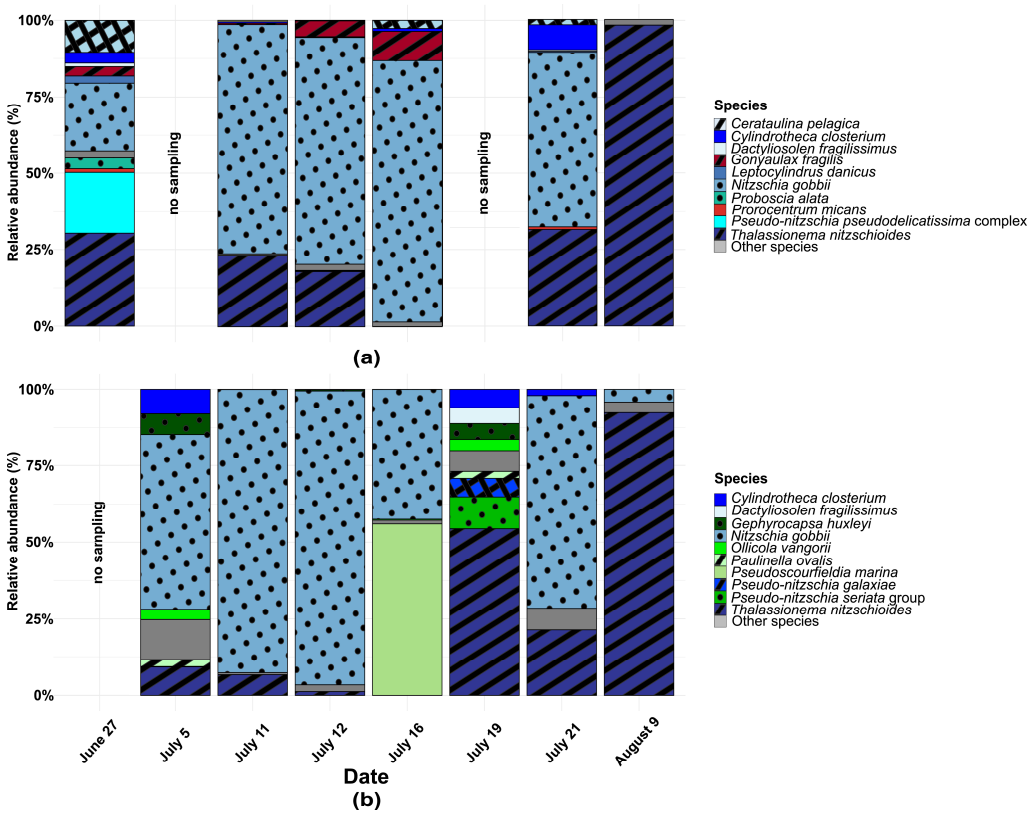

Figure 9. Relative abundance of the ten most abundant species identified by LM in mucilage (**a**) and surrounding water (**b**) samples.

Metabarcoding analysis of the 18S rRNA V4 region, using PR2 (Figure 10a) and SILVA (Figure 10b) as taxonomic reference databases, revealed that the species with the highest relative abundance in mucilage samples were represented by *Cylindrotheca closterium* (PR2 and SILVA), *Cyclotella choctawhatcheeana* Prasad (Mediophyceae) (SILVA), and *Pleurosigma planctonicum* A. Cleve (Bacillariophyceae) (SILVA). Among dinoflagellates, both databases assigned sequences to *Alexandrium margalefii* Balech (Dinophyceae) and *Gonyaulax fragilis* as most abundant. Other identified dinoflagellates species included *Pelagodinium bei* (H.J. Spero) Siano, Montresor, Probert and Vargas (Dinophyceae) (PR2), *Pseliodinium fusus* (F. Schütt) F. Gómez (Dinophyceae) (PR2 and SILVA), *Wangodinium sinense* Z. Luo, Zhangxi Hu, Yingzhong Tang and H.F. Gu (Dinophyceae) (PR2 and SILVA), and *Karlodinium veneficum* (D. Ballantine) J. Larsen (Dinophyceae) (SILVA). Among phytoflagellates, PR2 enabled the identification of *Mamiella gilva* Parke and Rayns (Mamiellophyceae), *Tetraselmis convolutae* (Parke and Manton) R.E. Norris, Hori and Chihara, (Chlorodendrophyceae), and *Tetraselmis verrucosa* f. *rubens* (Butcher) Hori, Norris and Chihara (Chlorodendrophyceae), whereas SILVA assigned sequences to *Picochlorum maculatum* (Butcher) Henley, Hironaka, Guillou, M. Buchheim, J. Buchheim, M. Fawley and K. Fawley (Trebouxiophyceae), and *Tetraselmis marina* (Cienkowski) R.E. Norris, Hori and Chihara (Chlorodendrophyceae).

3.3. Comparison Between Gulf of Trieste and Conero Riviera

Temporal changes in microalgae community composition were investigated in the Gulf of Trieste (Figure 11) and the Conero Riviera (Figure 12) both in the mucilage and surrounding water samples. These analyses were performed through MB of the V4 region, and, additionally, only for the Conero Riviera samples, of the V9 region.

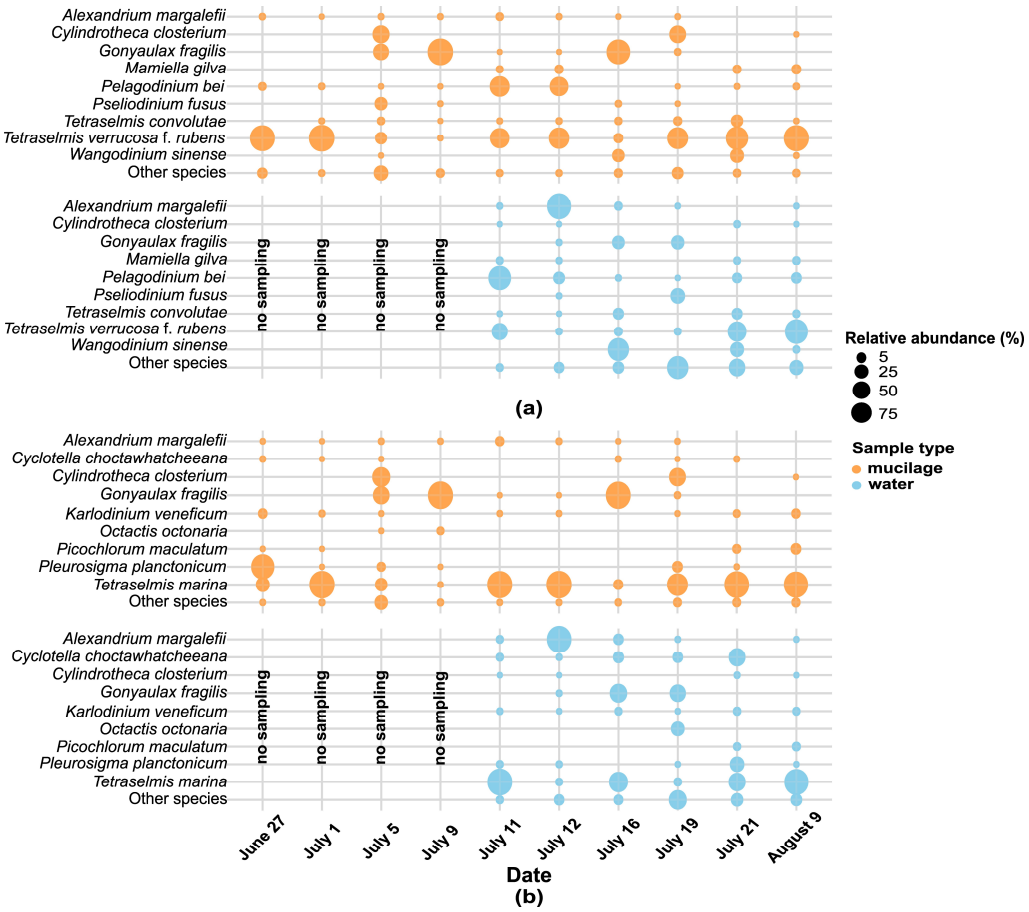

Figure 10. Relative abundance of dominant species in mucilage (orange) and surrounding water (light blue) samples obtained with MB using V4 marker and PR2 (**a**) and SILVA (**b**) databases.

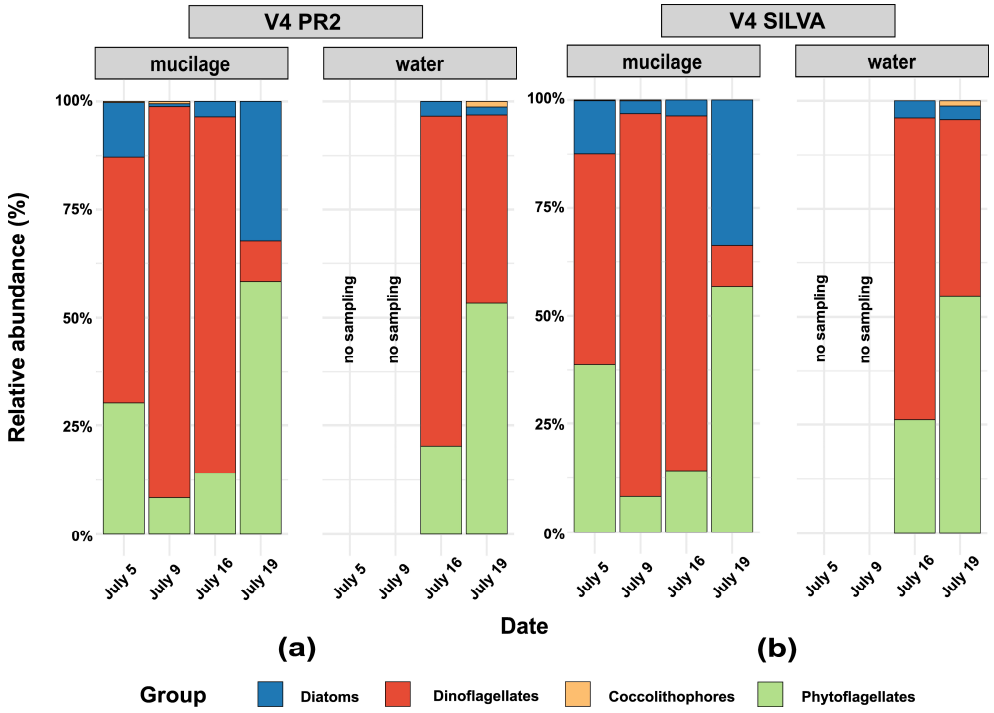

Figure 11. Relative abundance (%) of phytoplankton groups in mucilage and surrounding water samples from the Gulf of Trieste based on metabarcoding analyses using the V4 region and the two reference databases, PR2 (**a**) and SILVA (**b**), across sampling dates.

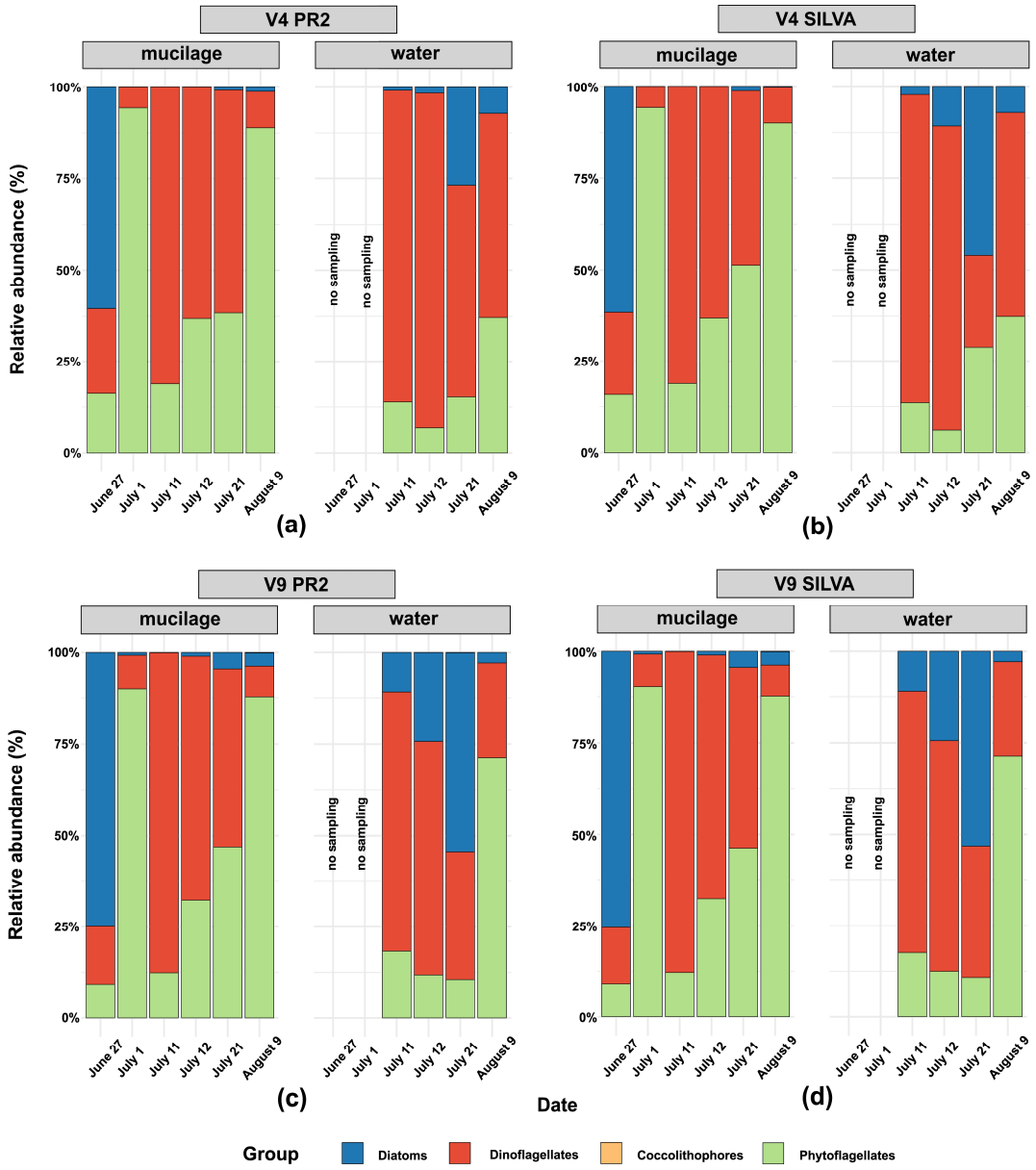

Figure 12. Relative abundance (%) of phytoplankton groups in mucilage and surrounding water samples from the Conero Riviera based on metabarcoding obtained with two genetic markers V4 (**a**,**b**) and V9 (**c**,**d**) with two reference databases (PR2 and SILVA) across sampling dates.

In the mucilage samples collected from the Gulf of Trieste it was observed that the relative abundance of phytoflagellates and diatoms increased over time. The abundance of phytoflagellates increased from 30–38% to 57–58% (depending on the database used), while diatoms increased from 12% to 32–34%. Conversely, dinoflagellates, which were dominant in the early sampling (until ~90% on 9 July), declined to 9% at the end. Coccolithophores, on the other hand, were consistently detected at very low proportions throughout the sampling period.

Similar trends were observed in the Conero Riviera where phytoflagellates generally increased over time (from 17 to 90%), with no substantial differences between the two markers and databases. Although a prominent peak occurred on 1 July (94%) the overall temporal pattern was characterized by a progressive increase in phytoflagellate relative abundance toward the end of the sampling period. Dinoflagellates and phytoflagellates were the dominant groups in both sample types; however, diatoms reached their maximum

relative abundance on the 27 June (60%). This pattern differs from that observed in the Gulf of Trieste. In contrast, and consistently with the findings in the Gulf of Trieste, coccolithophores occurred only at very low relative abundances across all samples. No substantial differences were observed in the composition of the samples when the V9 marker was used.

4. Discussion

In this study, an integrated approach that combines microscopy and metabarcoding was used for the first time to characterize microalgal communities within the mucilage aggregates of the Northern Adriatic Sea. The microalgal group composition as obtained by the two methodological approaches was different: LM identified phytoflagellates and diatoms as the most abundant groups, whereas phytoflagellates and dinoflagellates dominated according to MB. This discrepancy can be attributed first to methodological biases. MB may overestimate dinoflagellate relative abundance due to their high gene copy numbers related to their large genome [59,78], while LM analyses may underestimate them because formalin fixation often damages the thecae, making microscopic identification difficult. Moreover, MB revealed a greater diversity within phytoflagellates group compared to LM, as expected, since LM identification for this artificial group is generally limited to the class level. Nevertheless, LM remains essential for quantifying microalgal abundance. Some taxa clearly observed by LM, such as *Dactyliosolen blavyanus*, *Gonyaulax fragilis*, *Podolampas palmipes* F. Stein (Dinophyceae), *Protoperidinium bipes*, and *Tripos fusus* (Ehrenberg) F. Gómez (Dinophyceae), were not detected by MB. This detection failure can be linked to the high concentration of Extracellular Polymeric Substances (EPS) that form the mucilage, which significantly interferes with DNA extraction efficiency, purification, and PCR amplification [79]. Conversely, MB detected several additional taxa that were not observed by LM, including cryptic, small, or low abundance taxa that are difficult to identify with microscopy. Given that mucilage acts as an aggregator of organic material, it is possible that the detection of some species can be related to the presence of detrital DNA only, as also suggested by the numerous broken thecae, attributed to *G. fragilis*, that were found in the mucilage. Indeed, extracellular DNA, including detrital DNA, is known to persist in marine environments and can contribute to eDNA signals even in the absence of living cells [80,81].

The presence of mucus, besides interfering with MB analysis, hinders the counting under LM as it can cover the cells, change the microscopic focal plane, and impose the analysis of low-volume sub-samples. In this context, SEM observations provided additional support for species identification, particularly for critical genera or species that are difficult to resolve with LM alone, by revealing fine taxonomic characters and clarifying morphological features obscured also by the mucus.

The temporal trend of microalgal composition was similar in both sampling areas, where it was observed that phytoflagellates tend to increase over time. This pattern may be linked to the senescence of the aggregates, which can release nutrients and promote taxa with faster growth rates [29]. Indeed, microalgal communities are highly dynamic and likely respond to environmental drivers such as nutrient availability, hydrodynamics, and the aging of mucilage aggregates [53,82]. The very low relative abundance of coccolithophores across all stations, as observed through MB, may reflect the methodological limitations of MB, specifically the underrepresentation of these organisms in the reference databases used (SILVA and PR2) [58]. Species detected by MB such as *Alexandirum margalefii*, *Cylindrotheca closterium* and *Gonyaulax fragilis* have also been reported in mucilage of the Sea of Marmara using the same approach [54,55]. Furthermore, MB confirmed the presence of most abundant species already detected by microscopy analysis such as *Cylindrotheca*

closterium and *Gonyaulax fragilis*, which are identified at the species level by both methods. However, MB did not identify *Nitzschia gobbii* at the species level, only confirming the presence of the genus *Nitzschia*. This absence is most certainly linked to the lack of the V4 and V9 regions of the 18S rRNA gene for this species in the reference database. MB with SILVA as the taxonomic reference database also revealed a high relative abundance of *Pleurosigma planctonicum*, as LM and SEM only allowed for the identification of *Pleurosigma* at genus level. Moreover, MB provided higher taxonomic resolution within specific groups such as dinoflagellates, revealing species undetected by microscopy (e.g., *Karlodinium veneficum*, *Pseliodinium fusus*, and *Wangodinium sinense*). The same applies to phytoflagellates, with MB revealing a high relative abundance of chlorophytes such as *Tetraselmis* spp., which cannot be identified by LM. Differences were observed depending on the markers and databases used, likely due to differences in coverage and reference completeness among methods, especially at species level.

In agreement with previous findings, the mucilage aggregates exhibited significantly higher microalgal abundance than the surrounding water [29,49,53]. This has been explained considering that mucilage not only acts as a trap for detritus and microorganisms but also creates a favorable microenvironment for the active proliferation of protists and bacteria [29,36,53,82,83]. In this study, we further showed that in mucilage, species composition partially overlaps with that in the surrounding water. However, a clear imbalance was observed, with a higher number of genera and species in the surrounding water. These observations are consistent with previous studies reporting higher microbial diversity in the water than in mucilage [54]. This pattern may be explained, on the one hand, again by the polysaccharidic nature of the mucilage matrix which can interfere with the molecular procedures in MB and hinder accurate identification and counting at LM, potentially leading to an underestimation of diversity in mucilage samples. On the other hand, mucilage aggregates tend to become dominated over time by a limited number of opportunistic species, such as *Thalassionema nitzschioides* [84], resulting in reduced biodiversity.

Overall, all these methodological biases and complementarity highlighted the necessity of adopting an integrated approach to describe microalgae diversity and dynamics within mucilage aggregates. Each method alone provides a partial perspective, whereas their integration allows cross validation of results, improves taxonomic resolution, and enhances understanding of species dynamics linked to this complex phenomenon in agreement with studies that have previously used MB and LM to investigate mucilage [54].

Since the first studies in the 18th century, researchers have tried to identify the organisms responsible of the mucilage phenomenon by observing samples at the microscope, and in turn, many species have been suspected as main actors [20]. During the huge episodes in the 2000s in the NAS, it was indicated that *Gonyaulax fragilis* played a key role in mucilage formation through the production of extracellular polysaccharides, the main component of the mucus, which are released following the fragmentation of the thecae [41,85]. The hypothesis about a primary involvement of *G. fragilis* in mucus production is sustained by (i) the observation of its cells in the very early stage of the phenomenon, (ii) the occurrence of blooms of *G. fragilis* only in the years when mucilage appeared (in the past it has reached concentrations up to 3,400,000 cells/L) [85], (iii) the chemical composition of mucus produced by *G. fragilis* in culture conditions corresponds to that of mucilage [85], and (iv) the quantity and the aspect of mucus produced by *G. fragilis* under experimental conditions does reflect that of natural mucilage samples (Pistocchi pers. comm.). From this study, LM analysis revealed a high abundance of *Gonyaulax fragilis* at the beginning and throughout the mucilage event, while only a few cells or fragmented thecae were observed at the end of the sampling. Notably, the presence of this species was also detected by MB, but not at the onset of the phenomenon, as clearly observed through LM.

Although it is not possible to demonstrate beyond any reasonable doubt the functional role of *Gonyaulax fragilis* in mucilage formation, our results confirm its presence within mucilage aggregates throughout the event. However, to confirm the hypothesis of a possible involvement of this species in the mucilage production, sampling should ideally start just before the onset of mucilage formation to capture potential community shifts in the initial bloom dynamics.

Among diatoms, in both study areas, *Cylindrotheca closterium*, *Nitzschia gobbii*, *Nitzschia* spp., and *Thalassionema nitzschioides* were the dominant species, especially in older aggregates, in agreement with previous observations [36,53,84,86]. These species have been previously reported as mucus producers [37,86,87], and some authors considered them as potential contributors to mucilage formation [86]. Furthermore, it is widely recognized that mucilage aggregates offer a substratum very suitable for microalgal growth, favoring the development of a rich diatom community. We hypothesize that the presence of such diatoms could be explained considering that they find optimal growth conditions within the aggregates [29] and/or as they are physically trapped in the mucus. In our study, although we observed an increase in the relative abundance of these species in the days following the onset of the mucilage event, they were already present in significant numbers from the very beginning, alongside *Gonyaulax fragilis*, suggesting that the presence of mucilage benefits these species, as they become dominant over time [34,36,41,84–86].

5. Conclusions

This study represents the first characterization of mucilage-associated microalgal communities in the NAS using an integrated methodological approach. Although the sampling design was affected by the unpredictable nature of the phenomenon, our results highlighted the utility of adopting multidisciplinary and integrative approaches to investigate microalgal composition, abundance, and temporal dynamics within mucilage aggregates, particularly considering the analytical challenges caused by the mucilaginous matrix, which can interfere with single methods. By integrating complementary approaches, methodological limitations were mitigated leading to more robust and reliable results. Our findings confirm the dominance of key microalgal species previously associated with mucilage and provide new insights into their temporal succession. Given the ecological and economic impacts of mucilage events on marine ecosystems, fisheries, and coastal activities, further multidisciplinary studies will be crucial to unravel the mechanisms driving mucilage development and its ecological implications.

Supplementary Materials: The following supporting information can be downloaded at: https://www.mdpi.com/article/10.3390/phycology6010005/s1, Table S1: Abundance (cells/L) and relative abundances (%) of phytoplankton groups determined by microscopy analysis; Table S2: Species detected by metabarcoding (V4 PR2, V4 SILVA, V9 PR2, V9 SILVA) and light microscopy in mucilage and surrounding water samples; Table S3: Genus detected by metabarcoding (V4 PR2, V4 SILVA, V9 PR2, V9 SILVA) in mucilage and surrounding water samples.

Author Contributions: Conceptualization, C.T. and S.A.; methodology, M.U., J.F., T.T.D. and P.M.; software, F.N. and M.U.; validation, S.A.; formal analysis, M.U., F.C., J.F., T.T.D., P.M., T.R. and C.S.; investigation, M.U., F.C., J.F., T.T.D. and P.M.; resources, S.A., F.C., P.M. and C.T.; data curation, M.U., F.C., J.F., T.T.D., P.M., F.N., T.R., A.T., G.M. and C.S.; writing—original draft preparation, M.U.; writing—review and editing, C.T., S.A., F.C., J.F., T.T.D. and P.M.; visualization M.U.; supervision, C.T., S.A., F.C., J.F., T.T.D. and P.M.; project administration, S.A.; funding acquisition, S.A. All authors have read and agreed to the published version of the manuscript.

Funding: This work was partially funded under the National Recovery and Resilience Plan (NRRP), Mission 4 Component C2 Investment 1.1—Call for tender D.D. 104 of 2 February 2022 of Italian

Ministry of University and Research funded by the European Union—NextGenerationEU, Award Number: Project code 2022KZLJZH, Concession Decree D.D. 1015 of 7 July 2023 adopted by the Italian Ministry of University and Research, CUP I53D23003260006, Project title: Emerging toxins in Italian seas and risks for human health (Tox-IT). This work has also been funded by the National Biodiversity Future Center—NBFC, funded under the National Recovery and Resilience Plan, Mission 4 Component 2 Investment 1.4—Call for tender No. 3138 of 16 December 2021, rectified by Decree n.3175 of 18 December 2021 of Italian Ministry of University and Research funded by the European Union—NextGenerationEU (Project code CN_00000033, Concession Decree No. 1034 of 17 June 2022 adopted by the Italian Ministry of University and Research). This work was also supported by the Slovenian Research and Innovation Agency (core funding P1-0237).

Data Availability Statement: The original contributions presented in this study are included in the article/Supplementary Materials. Further inquiries can be directed to the corresponding author.

Acknowledgments: Authors thank Daniela Fornasaro for microscopy-based microalgal identification and enumeration at the C1-LTER station. The authors also thank the reviewers for their constructive comments, which greatly contributed to improving the quality of this work.

Conflicts of Interest: The authors declare no conflicts of interest.

Abbreviations

The following abbreviations are used in this manuscript:

NAS	Northern Adriatic Sea
LM	Light microscopy
SEM	Scanning electron microscopy
MB	Metabarcoding
HAB	Harmful Algal Bloom
ASVs	Amplicon sequence variants

References

1. Campanelli, A.; Grilli, F.; Paschini, E.; Marini, M. The influence of an exceptional Po River flood on the physical and chemical oceanographic properties of the Adriatic Sea. *Dyn. Atmos. Oceans* **2011**, *52*, 284–297. [CrossRef]
2. Djakovac, T.; Supić, N.; Bernardi Aubry, F.; Degobbis, D.; Giani, M. Mechanisms of hypoxia frequency changes in the northern Adriatic Sea during the period 1972–2012. *J. Mar. Syst.* **2015**, *141*, 179–189. [CrossRef]
3. Grilli, F.; Accoroni, S.; Acri, F.; Aubry, F.B.; Bergami, C.; Cabrini, M.; Campanelli, A.; Giani, M.; Guicciardi, S.; Marini, M.; et al. Seasonal and interannual trends of oceanographic parameters over 40 years in the northern Adriatic Sea in relation to nutrient loadings using the EMODnet chemistry data portal. *Water* **2020**, *12*, 2280. [CrossRef]
4. Penna, N.; Capellacci, S.; Ricci, F. The influence of the Po River discharge on phytoplankton bloom dynamics along the coastline of Pesaro (Italy) in the Adriatic Sea. *Mar. Pollut. Bull.* **2004**, *48*, 321–326. [CrossRef] [PubMed]
5. Brush, M.J.; Giani, M.; Totti, C.; Testa, J.M.; Faganeli, J.; Ogrinc, N.; Kemp, W.M.; Umani, S.F. Eutrophication, harmful algae, oxygen depletion, and acidification. In *Coastal Ecosystems in Transition: A Comparative Analysis of the Northern Adriatic and Chesapeake Bay*, 1st ed.; Malone, T.C., Malej, A., Faganeli, J., Eds.; Geophysical Monograph 256; John Wiley & Sons: Washington, DC, USA; Hoboken, NJ, USA, 2020; pp. 75–104.
6. Artegiani, A.; Paschini, E.; Russo, A.; Bregant, D.; Raicich, F.; Pinardi, N. The Adriatic Sea general circulation. Part I: Air–sea interactions and water mass structure. *J. Phys. Oceanogr.* **1997**, *27*, 1492–1514. [CrossRef]
7. Accoroni, S.; Romagnoli, T.; Colombo, F.; Pennesi, C.; Di Camillo, C.G.; Marini, M.; Battocchi, C.; Ciminiello, P.; Dell'Aversano, C.; Dello Iacovo, E.; et al. *Ostreopsis* cf. *ovata* bloom in the northern Adriatic Sea during summer 2009: Ecology, molecular characterization and toxin profile. *Mar. Pollut. Bull.* **2011**, *62*, 2512–2519. [CrossRef]
8. Henigman, U.; Mozetič, P.; Francé, J.; Knific, T.; Vadnjal, S.; Dolenc, J.; Kirbiš, A.; Biasizzo, M. Okadaic acid as a major problem for the seafood safety (*Mytilus galloprovincialis*) and the dynamics of toxic phytoplankton in the Slovenian coastal sea (Gulf of Trieste, Adriatic Sea). *Harmful Algae* **2024**, *135*, 102632. [CrossRef]
9. Zingone, A.; Escalera, L.; Aligizaki, K.; Fernández-Tejedor, M.; Ismael, A.; Montresor, M.; Mozetič, P.; Taş, S.; Totti, C. Toxic marine microalgae and noxious blooms in the Mediterranean Sea: A contribution to the global HAB status report. *Harmful Algae* **2021**, *102*, 101843. [CrossRef]
10. Boni, L. Red tides off the coast of Emilia Romagna (northwestern Adriatic Sea) from 1975 to 1982. *Inf. Bot. Ital.* **1983**, *15*, 18–23.

11. De Lazzari, A.; Berto, D.; Cassin, D.; Boldrin, A.; Giani, M. Influence of winds and oceanographic conditions on the mucilage aggregation in the northern Adriatic Sea in 2003–2006. *Mar. Ecol.* **2008**, *29*, 469–482. [CrossRef]
12. Giani, M.; Rinaldi, A.; Degobbis, D. Mucilages in the Adriatic and Tyrrhenian Sea: An introduction. *Sci. Total Environ.* **2005**, *353*, 3–9. [CrossRef] [PubMed]
13. Revelante, N.; Gilmartin, M. The phytoplankton composition and population enrichment in gelatinous "macroaggregates" in the Northern Adriatic during the summer of 1989. *J. Exp. Mar. Biol. Ecol.* **1991**, *146*, 217–233. [CrossRef]
14. Rinaldi, A.; Vollenweider, R.A.; Montanari, G.; Ferrari, C.R.; Ghetti, A. Mucilages in Italian Seas: The Adriatic and Tyrrhenian Seas, 1988–1991. *Sci. Total Environ.* **1995**, *165*, 165–183. [CrossRef]
15. Stachowitsch, M.; Fanuko, N.; Richter, M. Mucus aggregates in the Adriatic Sea: An overview of stages and occurrences. *Mar. Ecol.* **1990**, *11*, 327–350. [CrossRef]
16. Turk, V.; Hagström, Å.; Kovač, N.; Faganeli, J. Composition and function of mucilage macroaggregates in the northern Adriatic. *Aquat. Microb. Ecol.* **2010**, *61*, 279–289. [CrossRef]
17. Isinibilir, M.; Yüksel, E.; Martell, L.; Topçu, N.E. No escape from the mucilage impact: Even opportunistic Hydroids were affected in the catastrophic mucilage of 2021 in the Sea of Marmara. *Reg. Stud. Mar. Sci.* **2024**, *77*, 103678. [CrossRef]
18. Giani, M.; Berto, D.; Cornello, M.; Sartoni, G.; Rinaldi, A. *Le Mucillagini nell'Adriatico e nel Tirreno*; Quaderni dell'ICRAM; ICRAM: Rome, Italy, 2005.
19. Dagsuyu, E.; Can-Tuncelli, I.; Yanardag, R.; Erkan, N.; Dogruyol, H.; Ulusoy, S.; Ozden, O.; Mol, S.; Tosun, S.Y.; Ucok, D. Environmental stress responses to marine mucilage: Oxidative damage in economically important seafood from the Sea of Marmara. *Environ. Pollut.* **2025**, *374*, 126266. [CrossRef]
20. Fonda Umani, S.; Ghirardelli, E.; Ferrante, M. *Gli Episodi di "Mare Sporco" nell'Adriatico dal 1729 ai Giorni Nostri*; Regione Friuli-Venezia Giulia: Trieste, Italy, 1989.
21. Totti, C.; Cavolo, F.; Marzocchi, M.; Solazzi, A. Popolamenti fitoplanctonici durante il fenomeno del "Mare Sporco" in Adriatico settentrionale (estate 1989). *Quad. Is. Ric. Pesca Marittima* **1993**, *5*, 99–118.
22. ARPAE Emilia-Romagna. *Qualità Ambientale delle Acque Marine in Emilia-Romagna: Rapporto Annuale 2024*; ARPAE Emilia-Romagna: Bologna, Italy, 2024.
23. Faganeli, J.; Mohar, B.; Kofol, R.; Pavlica, V.; Marinšek, T.; Rozman, A.; Kovač, N.; Vuk, A.Š. Nature and lability of northern Adriatic macroaggregates. *Mar. Drugs* **2010**, *8*, 2480–2492. [CrossRef]
24. Kovač, N.; Viers, J.; Faganeli, J.; Bajt, O.; Pokrovsky, O.S. Elemental composition of plankton exometabolites (mucous macroaggregates): Control by biogenic and lithogenic components. *Metabolites* **2023**, *13*, 726. [CrossRef]
25. Kovač, N.; Mozetič, P.; Trichet, J.; Défarge, C. Phytoplankton composition and organic matter organization of mucous aggregates by means of light and cryo-scanning electron microscopy. *Mar. Biol.* **2005**, *147*, 261–271. [CrossRef]
26. Bongiorni, L.; Armeni, M.; Corinaldesi, C.; Dell'Anno, A.; Pusceddu, A.; Danovaro, R. Viruses, prokaryotes and biochemical composition of organic matter in different types of mucilage aggregates. *Aquat. Microb. Ecol.* **2007**, *49*, 15–23. [CrossRef]
27. Decho, A.W.; Herndl, G.J. Microbial activities and the transformation of organic matter within mucilaginous material. *Sci. Total Environ.* **1995**, *165*, 33–42. [CrossRef]
28. Zoppini, A.; Puddu, A.; Fazi, S.; Rosati, M.; Sist, P. Extracellular enzyme activity and dynamics of bacterial community in mucilaginous aggregates of the northern Adriatic Sea. *Sci. Total Environ.* **2005**, *353*, 270–286. [CrossRef]
29. Del Negro, P.; Crevatin, E.; Larato, C.; Ferrari, C.; Totti, C.; Pompei, M.; Giani, M.; Berto, D.; Fonda Umani, S. Mucilage microcosms. *Sci. Total Environ.* **2005**, *353*, 258–269. [CrossRef]
30. Simon, M.; Grossart, H.; Schweitzer, B.; Ploug, H. Microbial ecology of organic aggregates in aquatic ecosystems. *Aquat. Microb. Ecol.* **2002**, *28*, 175–211. [CrossRef]
31. Russo, A.; Maccaferri, S.; Djakovac, T.; Precali, R.; Degobbis, D.; Deserti, M.; Paschini, E.; Lyons, D.M. Meteorological and oceanographic conditions in the northern Adriatic Sea during the period June 1999–July 2002: Influence on the mucilage phenomenon. *Sci. Total Environ.* **2005**, *353*, 24–38. [CrossRef]
32. Vilibić, I.; Terzić, E.; Vrdoljak, I.; Dominović Novković, I.; Vodopivec, M.; Ciglenečki, I.; Djakovac, T.; Hamer, B. Extraordinary mucilage event in the northern Adriatic in 2024—A glimpse into the future climate? *Estuar. Coast. Shelf Sci.* **2025**, *317*, 109222. [CrossRef]
33. Danovaro, R.; Fonda Umani, S.; Pusceddu, A. Climate change and the potential spreading of marine mucilage and microbial pathogens in the Mediterranean Sea. *PLoS ONE* **2009**, *4*, e7006. [CrossRef]
34. Balkis, N.; Atabay, H.; Türetgen, I.; Albayrak, S.; Balkis, H.; Tüfekçi, V. Role of single-celled organisms in mucilage formation on the shores of Büyükada Island (the Marmara Sea). *J. Mar. Biol. Assoc. U. K.* **2011**, *91*, 771–781. [CrossRef]
35. MacKenzie, L.; Sims, I.; Beuzenberg, V.; Gillespie, P. Mass Accumulation of mucilage caused by dinoflagellate polysaccharide exudates in Tasman Bay, New Zealand. *Harmful Algae* **2002**, *1*, 69–83. [CrossRef]
36. Tüfekçi, V.; Balkis, N.; Polat Beken, Ç.; Ediger, D.; Mantıkçı, M. Phytoplankton composition and environmental conditions of the mucilage event in the Sea of Marmara. *Turk. J. Biol.* **2010**, *34*, 199–210. [CrossRef]

37. Alcoverro, T.; Conte, E.; Mazzella, L. Production of mucilage by the Adriatic epipelic diatom *Cylindrotheca closterium* (Bacillariophyceae) under nutrient limitation. *J. Phycol.* **2000**, *36*, 1087–1095. [CrossRef]
38. Haug, A.; Myklestad, S. Polysaccharides of marine diatoms with special reference to *Chaetoceros* species. *Mar. Biol.* **1976**, *34*, 217–222. [CrossRef]
39. Myklestad, S.M. Release of extracellular products by phytoplankton with special emphasis on polysaccharides. *Sci. Total Environ.* **1995**, *165*, 155–164. [CrossRef]
40. Myklestad, S. Production of carbohydrates by marine planktonic diatoms. II. Influence of the NP ratio in the growth medium on the assimilation ratio, growth rate, and production of cellular and extracellular carbohydrates by *Chaetoceros affinis* var. *willei* (Gran) Hustedt and *Skeletonema costatum* (Grev.) Cleve. *J. Exp. Mar. Biol. Ecol.* **1977**, *29*, 161–179. [CrossRef]
41. Pompei, M.; Mazziotti, C.; Guerrini, F.; Cangini, M.; Pigozzi, S.; Benzi, M.; Palamidesi, S.; Boni, L.; Pistocchi, R. Correlation between the presence of *Gonyaulax fragilis* (Dinophyceae) and the mucilage phenomena of the Emilia-Romagna coast (northern Adriatic Sea). *Harmful Algae* **2003**, *2*, 301–316. [CrossRef]
42. Guerrini, F.; Mazzotti, A.; Boni, L.; Pistocchi, R. Bacterial-algal interactions in polysaccharide production. *Aquat. Microb. Ecol.* **1998**, *15*, 247–253. [CrossRef]
43. Pistocchi, R.; Guerrini, F.; Balboni, V.; Boni, L. Copper toxicity and carbohydrate production in the microalgae *Cylindrotheca fusiformis* and *Gymnodinium* sp. *Eur. J. Phycol.* **1997**, *32*, 125–132. [CrossRef]
44. Doğan, O.; Örün, A.D.; Bilgin, R.; İşinibilir, M. Using the metabarcoding approach for characterization of community diversity in mucilage in the Sea of Marmara. In *Ecological Changes in the Sea of Marmara*; İşinibilir, M., Kıdeyş, A.E., Malej, A., Eds.; Istanbul University Press: Istanbul, Turkey, 2024; pp. 635–660.
45. Nikolaidis, G.; Aligizaki, K.; Koukaras, K.; Moschandreou, K. Mucilage phenomena in the north Aegean Sea, Greece: Another harmful effect of dinoflagellates? In Proceedings of the 12th International Conference on Harmful Algae, Copenhagen, Denmark, 4–8 September 2006; pp. 4–8.
46. Hurley, D.E. *The "Nelson Slime": Observations on Past Occurrences*; NZOI Oceanographic Summary; New Zealand Oceanographic Institute: Wellington, New Zealand, 1982; Volume 11.
47. Innamorati, M. Hyperproduction of mucilages by micro and macro algae in the Tyrrhenian Sea. *Sci. Total Environ.* **1995**, *165*, 65–81. [CrossRef]
48. Gundogdu, A.; Nalbantoglu, O.U.; Karis, G.; Sarikaya, I.; Erdogan, M.N.; Hora, M.; Aslan, H. Comparing microbial communities in mucilage and seawater samples: Metagenomic insights into mucilage formation in the Marmara Sea. *Environ. Sci. Pollut. Res.* **2024**, *31*, 58363–58374. [CrossRef]
49. Balkıs-Ozdelıce, N.; Durmuş, T.; Balcı, M. A preliminary study on the intense pelagic and benthic mucilage phenomenon observed in the Sea of Marmara. *IJEGEO* **2021**, *8*, 414–422. [CrossRef]
50. Cataletto, B.; Feoli, E.; Umani, S.F.; Monti, M.; Pecchiar, I. Analyses of the relationship between mucous aggregates and phytoplankton communities in the Gulf of Trieste (northern Adriatic Sea) by multivariate techniques. *Mar. Ecol.* **1996**, *17*, 291–307. [CrossRef]
51. Ergul, H.A.; Balkis-Ozdelice, N.; Koral, M.; Aksan, S.; Durmus, T.; Kaya, M.; Kayal, M.; Ekmekci, F.; Canli, O. The early stage of mucilage formation in the Marmara Sea during spring 2021. *J. Black Sea/Medit. Environ.* **2021**, *27*, 232–257.
52. Pettine, M.; Puddu, A.; Totti, C.; Zoppini, A.; Artegiani, A.; Pagnotta, R. Caratterizzazione chimica e biologica di mucillagini. *Biol. Mar. Suppl. Notiz. SIBM* **1993**, *1*, 39–42.
53. Totti, C.; Cangini, M.; Ferrari, C.; Kraus, R.; Pompei, M.; Pugnetti, A.; Romagnoli, T.; Vanucci, S.; Socal, G. Phytoplankton size-distribution and community structure in relation to mucilage occurrence in the northern Adriatic Sea. *Sci. Total Environ.* **2005**, *353*, 204–217. [CrossRef]
54. Akcaalan, R.; Ozbayram, E.G.; Kaleli, A.; Cam, A.O.; Koker, L.; Albay, M. Does environmental DNA reflect the actual phytoplankton diversity in the aquatic environment? Case study of marine mucilage in the Sea of Marmara. *Environ. Sci. Pollut. Res. Int.* **2023**, *30*, 72821–72831. [CrossRef]
55. Çelik, I.; Gülen, B.; Taş, P.; Geçgil, G.; Keskin, E. Identifying bacterial and eukaryotic communities related to marine mucilage with eDNA metabarcoding. *Microorganisms* **2024**, *12*, 318. [CrossRef]
56. Tzafesta, E.; Saccomanno, B.; Zangaro, F.; Vadrucci, M.R.; Specchia, V.; Pinna, M. DNA barcode gap analysis for multiple marker genes for phytoplankton species biodiversity in Mediterranean aquatic ecosystems. *Biology* **2022**, *11*, 1277. [CrossRef]
57. Andersson, A.; Zhao, L.; Brugel, S.; Figueroa, D.; Huseby, S. Metabarcoding vs microscopy: Comparison of methods to monitor phytoplankton communities. *ACS EST Water* **2023**, *3*, 2671–2680. [CrossRef]
58. Neri, F.; Ubaldi, M.; Accoroni, S.; Ricci, S.; Banchi, E.; Romagnoli, T.; Totti, C. Comparative analysis of phytoplankton diversity using microscopy and metabarcoding: Insights from an eLTER station in the northern Adriatic Sea. *Hydrobiologia* **2025**, *852*, 169–183. [CrossRef]

59. Piredda, R.; Tomasino, M.P.; D'Erchia, A.M.; Manzari, C.; Pesole, G.; Montresor, M.; Kooistra, W.H.C.F.; Sarno, D.; Zingone, A. Diversity and temporal patterns of planktonic protist assemblages at a Mediterranean Long Term Ecological Research site. *FEMS Microbiol. Ecol.* **2017**, *93*, fiw200. [CrossRef] [PubMed]
60. Throndsen, J. Preservation and Storage. In *Phytoplankton Manual. Monographs on Oceanographic Methodology*; Sournia, A., Ed.; UNESCO: Paris, France, 1978; pp. 69–74.
61. Kezlya, E.; Tseplik, N.; Kulikovskiy, M. Genetic markers for metabarcoding of freshwater microalgae: Review. *Biology* **2023**, *12*, 1038. [CrossRef] [PubMed]
62. Stoeck, T.; Bass, D.; Nebel, M.; Christen, R.; Jones, M.D.M.; Breiner, H.; Richards, T.A. Multiple marker parallel tag environmental DNA sequencing reveals a highly complex eukaryotic community in marine anoxic water. *Mol. Ecol.* **2010**, *19*, 21–31. [CrossRef]
63. Andrews, S. *FastQC: A Quality Control Tool for High Throughput Sequence Data*; Babraham Bioinformatics: Cambridge, UK, 2010.
64. Martin, M. Cutadapt removes adapter sequences from high-throughput sequencing reads. *EMBnet J.* **2011**, *17*, 10–12. [CrossRef]
65. Bolyen, E.; Rideout, J.R.; Dillon, M.R.; Bokulich, N.A.; Abnet, C.C.; Al-Ghalith, G.A.; Alexander, H.; Alm, E.J.; Arumugam, M.; Asnicar, F.; et al. Reproducible, interactive, scalable and extensible microbiome data science using QIIME 2. *Nat. Biotechnol.* **2019**, *37*, 852–857. [CrossRef]
66. Callahan, B.J.; McMurdie, P.J.; Rosen, M.J.; Han, A.W.; Johnson, A.J.A.; Holmes, S.P. DADA2: High-resolution sample inference from Illumina amplicon data. *Nat. Methods* **2016**, *13*, 581–583. [CrossRef]
67. Bokulich, N.A.; Kaehler, B.D.; Rideout, J.R.; Dillon, M.; Bolyen, E.; Knight, R.; Huttley, G.A.; Gregory Caporaso, J. Optimizing taxonomic classification of marker-gene amplicon sequences with QIIME 2's Q2-Feature-Classifier Plugin. *Microbiome* **2018**, *6*, 90. [CrossRef]
68. Guillou, L.; Bachar, D.; Audic, S.; Bass, D.; Berney, C.; Bittner, L.; Boutte, C.; Burgaud, G.; De Vargas, C.; Decelle, J.; et al. The Protist Ribosomal Reference Database (PR2): A catalog of unicellular eukaryote small sub-unit rRNA sequences with curated taxonomy. *Nucleic Acids Res.* **2012**, *41*, D597–D604. [CrossRef]
69. Quast, C.; Pruesse, E.; Yilmaz, P.; Gerken, J.; Schweer, T.; Yarza, P.; Peplies, J.; Glöckner, F.O. The SILVA ribosomal RNA gene database project: Improved data processing and web-based tools. *Nucleic Acids Res.* **2012**, *41*, D590–D596. [CrossRef]
70. Edler, L.; Elbrachter, M. The Utermöhl method for quantitative phytoplankton analysis. In *Microscopic and Molecular Methods for Quantitative Phytoplankton Analysis; Manuals and Guides*; Karlson, B., Cusack, C., Bresnan, E., Eds.; IOC UNESCO: Paris, France, 2010; Volume 55.
71. Hasle, G.R.; Syvertsen, E.E. Marine Diatoms. In *Identifying Marine Phytoplankton*; Tomas, C.R., Ed.; Academic Press: San Diego, CA, USA, 1997; pp. 5–385, ISBN 978-0-12-693018-4.
72. Guiry, M.D.; Guiry, G.M. *AlgaeBase. Global Electronic Publication, National University of Ireland, Galway*. Available online: https://www.algaebase.org (accessed on 19 December 2025).
73. McMurdie, P.J.; Holmes, S. Phyloseq: An R package for reproducible interactive analysis and graphics of microbiome census data. *PLoS ONE* **2013**, *8*, e61217. [CrossRef]
74. Altschul, S.F.; Gish, W.; Miller, W.; Myers, E.W.; Lipman, D.J. Basic local alignment search tool. *J. Mol. Biol.* **1990**, *215*, 403–410. [CrossRef]
75. Oksanen, J.; Blanchet, F.G.; Friendly, M.; Kindt, R.; Legendre, P.; McGlinn, D.; Minchin, P.R.; O'Hara, R.B.; Simpson, G.L.; Solymos, P.; et al. Vegan: Community Ecology Package, R Package Version 2.6-2, 2022. Available online: https://CRAN.R-project.org/package=vegan (accessed on 17 December 2025).
76. R Core Team. *R: A Language and Environment for Statistical Computing*; R Foundation for Statistical Computing: Vienna, Austria, 2023. Available online: https://www.R-project.org (accessed on 17 December 2025).
77. Wickham, H. *ggplot2: Elegant Graphics for Data Analysis*; Springer: New York, NY, USA, 2016. Available online: https://ggplot2.tidyverse.org (accessed on 17 December 2025).
78. Prokopowich, C.D.; Gregory, T.R.; Crease, T.J. The correlation between rDNA copy number and genome size in eukaryotes. *Genome* **2003**, *46*, 48–50. [CrossRef]
79. Japelaghi, R.H.; Haddad, R.; Garoosi, G.-A. Rapid and efficient isolation of high quality nucleic acids from plant tissues rich in polyphenols and polysaccharides. *Mol. Biotechnol.* **2011**, *49*, 129–137. [CrossRef] [PubMed]
80. Carini, P.; Marsden, P.J.; Leff, J.W.; Morgan, E.E.; Strickland, M.S.; Fierer, N. Relic DNA is abundant in soil and obscures estimates of soil microbial diversity. *Nat. Microbiol.* **2016**, *2*, 16242. [CrossRef] [PubMed]
81. Lennon, J.T.; Muscarella, M.E.; Placella, S.A.; Lehmkuhl, B.K. How, when, and where relic DNA affects microbial diversity. *mBio* **2018**, *9*, e00637-18. [CrossRef] [PubMed]
82. Reynolds, C.S. Variability in the provision and function of mucilage in phytoplankton: Facultative responses to the environment. *Hydrobiologia* **2007**, *578*, 37–45. [CrossRef]
83. Flander-Putrle, V.; Malej, A. The evolution and phytoplankton composition of mucilaginous aggregates in the northern Adriatic Sea. *Harmful Algae* **2008**, *7*, 752–761. [CrossRef]

84. Kraus, R.; Supić, N. Sea Dynamics Impacts on the Macroaggregates: A case study of the 1997 mucilage event in the Northern Adriatic. *Prog. Oceanogr.* **2015**, *138*, 249–267. [CrossRef]
85. Pistocchi, R.; Cangini, M.; Totti, C.; Urbani, R.; Guerrini, F.; Romagnoli, T.; Sist, P.; Palamidesi, S.; Boni, L.; Pompei, M. Relevance of the dinoflagellate *Gonyaulax fragilis* in mucilage formations of the Adriatic Sea. *Sci. Total Environ.* **2005**, *353*, 307–316. [CrossRef]
86. Najdek, M.; Blažina, M.; Djakovac, T.; Kraus, R. The role of the diatom *Cylindrotheca closterium* in a mucilage event in the northern Adriatic Sea: Coupling with high salinity water intrusions. *J. Plankton Res.* **2005**, *27*, 851–862. [CrossRef]
87. Allan, G.G.; Lewin, J.; Johnson, P.G. Marine polymers. IV diatom polysaccharides. *Bot. Mar.* **1972**, *15*, 102–108. [CrossRef]